Optimal Shape Design for the Viscous Incompressible Flow

Zhiming Gao, Yichen Ma

Optimal Shape Design for the Viscous Incompressible Flow*

Zhiming Gao† and Yichen Ma‡

January 17, 2007

Abstract. This paper is concerned with a numerical simulation of shape optimization in a two-dimensional viscous incompressible flow governed by Navier–Stokes equations with mixed boundary conditions containing the pressure. The minimization problem of total dissipated energy was established in the fluid domain. We derive the structures of shape gradient of the cost functional by using the differentiability of a minimax formulation involving a Lagrange functional with a function space parametrization technique. Finally a gradient type algorithm is effectively used for our problem.

Keywords. shape optimization; minimax principle; gradient algorithm; Navier–Stokes equations.

AMS (2000) subject classifications. 35B37, 35Q30, 49K35.

1 Introduction

The problem of finding the optimal design of a system for the viscous incompressible flow arises in many design problems in aerospace, automotive, hydraulic, ocean, structural, and wind engineering. In practise, engineers are interested in reducing the drag force in the wing of a plane or vehicle or in reducing the dissipation in channels, hydraulic values, etc.

The optimal shape design of a body subjected to the minimum dissipate viscous energy has been a challenging task for a long time, and it has been investigated by several authors. For instance, O.Pironneau in [16, 14] computes the derivative of the cost functional using normal variation approach; F.Murat and J.Simon in [15] use the formal calculus to deduce an expression for the derivative; J.A.Bello *et.al.* in [1, 2, 3] considered this problem theoretically in the case of Navier–Stokes flow by the formal calculus.

*This work was supported by the National Natural Science Fund of China under grant number 10671153.

†Corresponding author. School of Science, Xi'an Jiaotong University, P.O.Box 1844, Xi'an, Shaanxi, P.R.China, 710049. E–mail:dtgaozm@gmail.com.

‡School of Science, Xi'an Jiaotong University, Shaanxi, P.R.China, 710049. E-mail: ycma@mail.xjtu.edu.cn.

The previous references concern Dirichlet boundary conditions for the velocity. However, the velocity–pressure type boundary conditions must be introduced and it seems more realistic in many industrial applications, such as shape optimization of Aorto–Coronaric bypass anastomoses in biomedical engineering. Recently, H.Yagi and M. Kawahara in [20] study the optimal shape design for Navier–Stokes flow with boundary conditions containing the pressure using a discretize–then–differentiate approach. However, its proposed algorithm converges slowly. E.Katamine *et.al.*[13] use the differentiate–then–discretize approach with the formulae of material derivative to study such problem involving velocity–pressure type boundary conditions with Reynolds number up to 100.

In the present paper, we will use the so-called function space parametrization technique which was advocated by M.C.Delfour and J.-P.Zolésio to solving poisson equation with Dirichlet and Nuemann condition (see [6]). In our paper [8, 9, 10], we apply them to solve a Robin problem and shape reconstruction problems for Stokes and Navier–Stokes flow with Dirichlet boundary condition only involving the velocity, respectively.

However, in this paper we extend them to study the energy minimization problem for Navier–Stokes flow with velocity–pressure boundary conditions in despite of its lack of rigorous mathematical justification in case where the Lagrange formulation is not convex. We shall show how this theorem allows, at least formally to bypass the study of material derivative and obtain the expression of shape gradient for the given cost functional. Finally we will introduce an efficient numerical algorithm for the solution of such minimization problems and the numerical examples show that our proposed algorithm converges very fast.

This paper is organized as follows. In section 2, we briefly recall the velocity method which is used for the characterization of the deformation of the shape of the domain and give the description of the shape minimization problem for the Navier–Stokes flow with mixed type boundary conditions.

Section 3 is devoted to the computation of the shape gradient of the Lagrangian functional due to a minimax principle concerning the differentiability of the minimax formulation by function space parametrization technique.

Finally in section 4, we give its finite element approximation and propose a gradient type algorithm with some numerical examples to show that our theory could be very useful for the practical purpose and the proposed algorithm is efficient.

2 Preliminaries and statement of the problem

2.1 Elements of the velocity method

To our little knowledge, there are about three types of techniques to perform the domain deformation: J.Hadamard [12]'s normal variation method, the perturbation of the identity method by J.Simon [18] and the velocity method (see J.Cea[4] and J.-

P.Zolesio[6, 21]). We will use the velocity method which contains the others. In that purpose, we choose an open set D in $\mathbb{R}^N$ with the boundary ∂D piecewise C^k, and a velocity space $\boldsymbol{V} \in \mathrm{E}^k := C([0,\varepsilon];[\mathcal{D}^k(\bar{D})]^N)$, where ε is a small positive real number and $[\mathcal{D}^k(\bar{D})]^N$ denotes the space of all $k-$times continuous differentiable functions with compact support contained in D. The velocity field

$$\boldsymbol{V}(t)(x) = \boldsymbol{V}(t,x), \qquad x \in D, \quad t \geq 0$$

belongs to $[\mathcal{D}^k(\bar{D})]^N$ for each t. It can generate transformations $T_t(\boldsymbol{V})X = x(t,X)$ through the following dynamical system

$$\frac{\mathrm{d}x}{\mathrm{d}t}(t,X) = \boldsymbol{V}(t,x(t)), \qquad x(0,X) = X$$

with the initial value X given. We denote the "transformed domain" $T_t(\boldsymbol{V})(\Omega)$ by $\Omega_t(\boldsymbol{V})$ at $t \geq 0$, and also set its boundary $\Gamma_t := T_t(\Gamma)$.

There exists an interval $I = [0,\delta)$, $0 < \delta \leq \varepsilon$, and a one-to-one map T_t from $\bar{D}$ onto $\bar{D}$ such that

(i) $T_0 = \mathrm{I}$;

(ii) $(t,x) \mapsto T_t(x)$ belongs to $C^1(I;C^k(D))$ with $T_t(\partial D) = \partial D$;

(iii) $(t,x) \mapsto T_t^{-1}(x)$ belongs to $C(I;C^k(D))$.

Such transformation are well studied in [6].

Furthermore, for sufficiently small $t > 0$, the Jacobian J_t is strictly positive:

$$J_t(x) := \det|\mathrm{D}T_t(x)| = \det \mathrm{D}T_t(x) > 0,$$

where $\mathrm{D}T_t(x)$ denotes the Jacobian matrix of the transformation T_t evaluated at a point $x \in D$ associated with the velocity field $\boldsymbol{V}$. We will also use the following notation: $\mathrm{D}T_t^{-1}(x)$ is the inverse of the matrix $\mathrm{D}T_t(x)$, ${}^*\mathrm{D}T_t^{-1}(x)$ is the transpose of the matrix $\mathrm{D}T_t^{-1}(x)$. These quantities also satisfy the following lemma.

Lemma 2.1 *For any $\boldsymbol{V} \in E^k$, $\mathrm{D}T_t$ and J_t are invertible. Moreover, $\mathrm{D}T_t$, $\mathrm{D}T_t^{-1}$ are in $C^1([0,\varepsilon];[C^{k-1}(\bar{D})]^{N\times N})$, and J_t, J_t^{-1} are in $C^1([0,\varepsilon];C^{k-1}(\bar{D}))$.*

Now let $J(\Omega)$ be a real valued functional associated with any regular domain Ω, we say that the functional $J(\Omega)$ has a **Eulerian derivative** at Ω in the direction $\boldsymbol{V}$ if the limit

$$\lim_{t\searrow 0} \frac{1}{t}\left[J(\Omega_t) - J(\Omega)\right] := \mathrm{d}J(\Omega;\boldsymbol{V})$$

exists.

Furthermore, if the map $\boldsymbol{V} \mapsto \mathrm{d}J(\Omega;\boldsymbol{V}) : \mathrm{E}^k \to \mathbb{R}$ is linear and continuous, we say that J is **shape differentiable** at Ω. In the distributional sense we have

$$\mathrm{d}J(\Omega;\boldsymbol{V}) = \langle \nabla J, \boldsymbol{V}\rangle_{(\mathcal{D}^k(\bar{D})^N)'\times\mathcal{D}^k(\bar{D})^N}. \tag{2.1}$$

When J has a Eulerian derivative, we say that ∇J is the **shape gradient** of J at Ω.

Before closing this subsection, we introduce the following functional spaces which will be used in this paper:

$$
\begin{aligned}
H(\Omega) &:= \{\boldsymbol{u} \in H^1(\Omega)^N : \ \operatorname{div} \boldsymbol{u} = 0 \text{ in } \Omega,\ \boldsymbol{u} = 0 \text{ on } \Gamma_w \cup \Gamma_s,\ \boldsymbol{u} = \boldsymbol{g} \text{ on } \Gamma_u\},\\
V_g(\Omega) &:= \{\boldsymbol{u} \in H^2(\Omega)^N : \ \boldsymbol{u} = 0 \text{ on } \Gamma_w \cup \Gamma_s,\ \boldsymbol{u} = \boldsymbol{g} \text{ on } \Gamma_u\},\\
V_0(\Omega) &:= \{\boldsymbol{u} \in H^2(\Omega)^N : \ \boldsymbol{u} = 0 \text{ on } \Gamma_w \cup \Gamma_u \cup \Gamma_s\},\\
Q(\Omega) &:= \left\{ p \in H^1(\Omega) : \ \int_\Omega p \, \mathrm{d}x = 0 \ (\text{ if } \operatorname{meas}(\Gamma_d) = 0) \right\}.
\end{aligned}
$$

2.2 Formulation of the flow optimization problem

Let Ω be a region of $\mathbb{R}^2$ and we denote by Γ the boundary of Ω. We suppose that Ω is filled with a Newtonian incompressible viscous fluid of the kinematic viscosity ν. The flow of such a fluid is modeled by the following system of Navier–Stokes equations,

$$
-\operatorname{div} \sigma(\boldsymbol{y}, p) + \mathrm{D}\boldsymbol{y} \cdot \boldsymbol{y} = 0 \qquad \text{in } \Omega, \tag{2.2}
$$

$$
\operatorname{div} \boldsymbol{y} = 0 \qquad \text{in } \Omega, \tag{2.3}
$$

where $\boldsymbol{y}$ denotes the velocity field, p the pressure, and $\sigma(\boldsymbol{y}, p)$ the stress tensor defined by $\sigma(\boldsymbol{y}, p) := -p\mathrm{I} + 2\nu\varepsilon(\boldsymbol{y})$ with the rate of deformation tensor $\varepsilon(\boldsymbol{y}) := (\mathrm{D}\boldsymbol{y} + {}^*\mathrm{D}\boldsymbol{y})/2$, where ${}^*\mathrm{D}\boldsymbol{y}$ denotes the transpose of the matrix $\mathrm{D}\boldsymbol{y}$ and I denotes the identity tensor.

Equations (2.2) and (2.3) have to be completed by the following typical boundary conditions:

$$
\boldsymbol{y} = \boldsymbol{g} \quad \text{on } \Gamma_u \tag{2.4}
$$

$$
\boldsymbol{y} = 0 \quad \text{on } \Gamma_s \cup \Gamma_w \tag{2.5}
$$

$$
\sigma(\boldsymbol{y}, p) \cdot \boldsymbol{n} = \boldsymbol{h} \quad \text{on } \Gamma_d \tag{2.6}
$$

where $\boldsymbol{n}$ denotes the unit vector of outward normal on $\Gamma = \Gamma_u \cup \Gamma_d \cup \Gamma_w \cup \Gamma_s$, Γ_u is the inflow boundary, Γ_d the outflow boundary, Γ_w the boundary corresponding to the fluid wall and Γ_s is the boundary which is to be optimized. We also recall that the Reynolds number Re is classically defined by $\mathrm{Re} = UL/\nu$ with U a characteristic velocity and L a characteristic length.

For the existence and uniqueness of the solution of the Navier–Stokes system (2.2)–(2.6), we have the following results (see [19]).

Theorem 2.1 *Suppose that Ω is of class C^1. For the data*

$$
\boldsymbol{g} \in H^{3/2}(D)^N, \qquad \int_{\Gamma_u} \boldsymbol{g} \cdot \boldsymbol{n} \, \mathrm{d}s = 0; \qquad \boldsymbol{h} \in H^{1/2}(D)^N,
$$

there exists at least one $\boldsymbol{y} \in H(\Omega)$ and a distribution $p \in L^2(\Omega)$ on Ω such that (2.2)–(2.6) hold. Moreover, if ν is sufficiently large or $\boldsymbol{g}$ and $\boldsymbol{h}$ sufficiently small, there exists a unique solution $(\boldsymbol{y}, p) \in H(\Omega) \times L^2(\Omega)$ to the problem (2.2)–(2.6). In addition, if Ω is of class C^2, we have $(\boldsymbol{y}, p) \in V_g(\Omega) \times Q(\Omega)$.

Our goal is to optimize the shape of the domain Ω which minimizes a given cost functional depending on the fluid domain and the state. The cost functional may represent a given objective related to specific characteristic features of the flow (e.g., the deviation with respect to a given target pressure, the drag, the vorticity, $\cdots$).

We are interested in solving the total dissipation energy minimization problem

$$\min_{\Omega\in\mathcal{O}} J(\Omega) = 2\nu \int_\Omega |\varepsilon(\boldsymbol{y})|^2 \,\mathrm{d}x, \tag{2.7}$$

where the boundary $\Gamma_u \cup \Gamma_d \cup \Gamma_w$ is fixed and an example of the admissible set $\mathcal{O}$ is:

$$\mathcal{O} := \left\{ \Omega \subset \mathbb{R}^N : \ \Gamma_u \cup \Gamma_d \cup \Gamma_w \text{ is fixed, } \int_\Omega \mathrm{d}x = \text{constant} \right\}.$$

Corollary 2.1 ([17]) *Let Ω be of piecewise C^1, the minimization problem (2.7) has at least one solution with given area in two dimensions.*

3 Function space parametrization

In this section we derive the structure of the shape gradient for the cost functional $J(\Omega)$ by function space parametrization techniques in order to bypass the usual study of material derivative.

Let Ω be of class C^2, the weak formulation of (2.2)–(2.6) in mixed form is:

$$\begin{cases} \text{seek } (\boldsymbol{y}, p) \in V_g(\Omega) \times Q(\Omega) \text{ such that} \\ \int_\Omega [2\nu\varepsilon(\boldsymbol{y}) : \varepsilon(\boldsymbol{v}) + \mathrm{D}\boldsymbol{y}\cdot\boldsymbol{y}\cdot\boldsymbol{v} - p\,\mathrm{div}\,\boldsymbol{v}]\,\mathrm{d}x = \int_{\Gamma_d} \boldsymbol{h}\cdot\boldsymbol{v}\,\mathrm{d}s, \ \forall \boldsymbol{v} \in V_0(\Omega), \\ \int_\Omega \mathrm{div}\,\boldsymbol{y} q\,\mathrm{d}x = 0, \ \forall q \in Q(\Omega). \end{cases} \tag{3.1}$$

Where in the weak form (3.1), we have used the following lemma.

Lemma 3.1

$$2\int_\Omega \varepsilon(\boldsymbol{y}) : \varepsilon(\boldsymbol{v})\,\mathrm{d}x = -\int_\Omega (\Delta\boldsymbol{y} + \nabla\,\mathrm{div}\,\boldsymbol{y})\cdot\boldsymbol{v}\,\mathrm{d}x + 2\int_{\partial\Omega} \varepsilon(\boldsymbol{y})\cdot\boldsymbol{n}\cdot\boldsymbol{v}\,\mathrm{d}s.$$

Now we introduce the following Lagrange functional associated with (3.1) and (2.7):

$$G(\Omega, \boldsymbol{y}, p, \boldsymbol{v}, q) = J(\Omega) - L(\Omega, \boldsymbol{y}, p, \boldsymbol{v}, q), \tag{3.2}$$

where

$$L(\Omega, \boldsymbol{y}, p, \boldsymbol{v}, q) = \int_\Omega [2\nu\varepsilon(\boldsymbol{y}) : \varepsilon(\boldsymbol{v}) + \mathrm{D}\boldsymbol{y}\cdot\boldsymbol{y}\cdot\boldsymbol{v} - p\,\mathrm{div}\,\boldsymbol{v}]\,\mathrm{d}x - \int_{\Gamma_d} \boldsymbol{h}\cdot\boldsymbol{v}\,\mathrm{d}s - \int_\Omega \mathrm{div}\,\boldsymbol{y} q\,\mathrm{d}x.$$

The minimization problem (2.7) can be put in the following form

$$\min_{\Omega\in\mathcal{O}} \min_{(\boldsymbol{y},p)\in V_g(\Omega)\times Q(\Omega)} \max_{(\boldsymbol{v},q)\in V_0(\Omega)\times Q(\Omega)} G(\Omega, \boldsymbol{y}, p, \boldsymbol{v}, q), \tag{3.3}$$

We can use the minimax framework to avoid the study of the state derivative with respect to the shape of the domain. The Karusch-Kuhn-Tucker conditions will furnish

the shape gradient of the cost functional $J(\Omega)$ by using the adjoint system. Now let's establish the first optimality condition for the problem

$$\min_{(\boldsymbol{y},p)\in V_g(\Omega)\times Q(\Omega)} \max_{(\boldsymbol{v},q)\in V_0(\Omega)\times Q(\Omega)} G(\Omega,\boldsymbol{y},p,\boldsymbol{v},q). \tag{3.4}$$

Formally the adjoint equations are defined from the Euler–Lagrange equations of the Lagrange functional G. Clearly, the variation of G with respect to $(\boldsymbol{v},q)$ can recover the state system (3.1). On the other hand, in order to find the adjoint state system, we differentiate G with respect to p in the direction δp,

$$\frac{\partial G}{\partial p}(\Omega,\boldsymbol{y},p,\boldsymbol{v},q)\cdot\delta p=\int_\Omega \delta p\,\mathrm{div}\,\boldsymbol{v}\,\mathrm{d}x=0,$$

Taking δp with compact support in Ω gives

$$\mathrm{div}\,\boldsymbol{v}=0. \tag{3.5}$$

Then we differentiate G with respect to $\boldsymbol{y}$ in the direction $\delta\boldsymbol{y}$ and employ Green formula,

$$\begin{aligned}\frac{\partial G}{\partial \boldsymbol{y}}(\Omega,\boldsymbol{y},p,\boldsymbol{v},q)\cdot\delta\boldsymbol{y}=&\int_\Omega(-2\nu\Delta\boldsymbol{y}+\nu\Delta\boldsymbol{v}-\nabla q-{}^*\mathrm{D}\boldsymbol{y}\cdot\boldsymbol{v}+\mathrm{D}\boldsymbol{v}\cdot\boldsymbol{y})\cdot\delta\boldsymbol{y}\,\mathrm{d}x\\&-\int_{\partial\Omega}\sigma(\boldsymbol{v},q)\cdot\boldsymbol{n}\cdot\delta\boldsymbol{y}\,\mathrm{d}s+4\nu\int_{\partial\Omega}\varepsilon(\boldsymbol{y})\cdot\boldsymbol{n}\cdot\delta\boldsymbol{y}\,\mathrm{d}s-\int_{\partial\Omega}(\boldsymbol{y}\cdot\boldsymbol{n})(\boldsymbol{v}\cdot\delta\boldsymbol{y})\,\mathrm{d}s.\end{aligned}$$

Taking $\delta\boldsymbol{y}$ with compact support in Ω gives

$$-\nu\Delta\boldsymbol{v}+\nabla q+{}^*\mathrm{D}\boldsymbol{y}\cdot\boldsymbol{v}-\mathrm{D}\boldsymbol{v}\cdot\boldsymbol{y}=-2\nu\Delta\boldsymbol{y}. \tag{3.6}$$

Then varying $\delta\boldsymbol{y}$ on Γ_d gives

$$\sigma(\boldsymbol{v},q)\cdot\boldsymbol{n}+(\boldsymbol{y}\cdot\boldsymbol{n})\boldsymbol{v}-4\nu\varepsilon(\boldsymbol{y})\cdot\boldsymbol{n}=0,\qquad\text{on }\Gamma_d. \tag{3.7}$$

Finally we obtain the following adjoint state system

$$\begin{cases}-\mathrm{div}\,\sigma(\boldsymbol{v},q)+{}^*\mathrm{D}\boldsymbol{y}\cdot\boldsymbol{v}-\mathrm{D}\boldsymbol{v}\cdot\boldsymbol{y}=-2\nu\Delta\boldsymbol{y} & \text{in }\Omega\\ \mathrm{div}\,\boldsymbol{v}=0 & \text{in }\Omega\\ \sigma(\boldsymbol{v},q)\cdot\boldsymbol{n}+(\boldsymbol{y}\cdot\boldsymbol{n})\boldsymbol{v}-4\nu\varepsilon(\boldsymbol{y})\cdot\boldsymbol{n}=0, & \text{on }\Gamma_d\\ \boldsymbol{v}=0 & \text{on }\Gamma_u\cup\Gamma_w\cup\Gamma_s,\end{cases} \tag{3.8}$$

and its variational form

$$\begin{cases}\text{seek }(\boldsymbol{v},q)\in V_0(\Omega)\times Q(\Omega)\text{ such that }\forall(\boldsymbol{\varphi},\psi)\in V_0(\Omega)\times Q(\Omega),\\ \int_\Omega[2\nu\varepsilon(\boldsymbol{v}):\varepsilon(\boldsymbol{\varphi})+\mathrm{D}\boldsymbol{\varphi}\cdot\boldsymbol{y}\cdot\boldsymbol{v}+\mathrm{D}\boldsymbol{y}\cdot\boldsymbol{\varphi}\cdot\boldsymbol{v}-q\,\mathrm{div}\,\boldsymbol{\varphi}]\,\mathrm{d}x=4\nu\int_\Omega\varepsilon(\boldsymbol{y}):\varepsilon(\boldsymbol{\varphi})\,\mathrm{d}x,\\ \int_\Omega\mathrm{div}\,\boldsymbol{v}\psi\,\mathrm{d}x=0.\end{cases} \tag{3.9}$$

We employ the velocity method to modelize the domain deformations. We only perturb the boundary Γ_s and consider the mapping $T_t(\boldsymbol{V})$, the flow of the velocity field

$$\boldsymbol{V}\in V_{\mathrm{ad}}:=\{\boldsymbol{V}\in C^0(0,\tau;C^2(\mathbb{R}^N)^N):\ V=0\text{ in the neighorhood of }\Gamma_u\cup\Gamma_w\cup\Gamma_d\}.$$

We denote the perturbed domain $\Omega_t = T_t(\boldsymbol{V})(\Omega)$.

Our objective in this section is to study the derivative of $j(t)$ with respect to t, where

$$j(t) := \min_{(\boldsymbol{y}_t, p_t)\in V_g(\Omega_t)\times Q(\Omega_t)} \max_{(\boldsymbol{v}_t, q_t)\in V_0(\Omega_t)\times Q(\Omega_t)} G(\Omega_t, \boldsymbol{y}_t, p_t, \boldsymbol{v}_t, q_t), \tag{3.10}$$

$(\boldsymbol{y}_t, p_t)$ and $(\boldsymbol{v}_t, q_t)$ satisfy (3.1) and (3.9) on the perturbed domain Ω_t, respectively.

Unfortunately, the Sobolev space $V_g(\Omega_t)$, $V_0(\Omega_t)$, and $Q(\Omega_t)$ depend on the parameter t, so we need to introduce the so-called function space parametrization technique which consists in transporting the different quantities (such as, a cost functional) defined on the variable domain Ω_t back into the reference domain Ω which does not depend on the perturbation parameter t. Thus we can use differential calculus since the functionals involved are defined in a fixed domain Ω with respect to the parameter t.

To do this, we define the following parametrizations

$$\begin{aligned} V_g(\Omega_t) &= \{\boldsymbol{y}\circ T_t^{-1} :\ \boldsymbol{y}\in V_g(\Omega)\};\\ V_0(\Omega_t) &= \{\boldsymbol{v}\circ T_t^{-1} :\ \boldsymbol{v}\in V_0(\Omega)\};\\ Q(\Omega_t) &= \{p\circ T_t^{-1} :\ p\in Q(\Omega)\}. \end{aligned}$$

where "$\circ$" denotes the composition of the two maps.

Note that since T_t and T_t^{-1} are diffeomorphisms, these parametrizations can not change the value of the saddle point. We can rewrite (3.10) as

$$j(t) = \min_{(\boldsymbol{y},p)\in V_g(\Omega)\times Q(\Omega)} \max_{(\boldsymbol{v},q)\in V_0(\Omega)\times Q(\Omega)} G(\Omega_t, \boldsymbol{y}\circ T_t^{-1}, p\circ T_t^{-1}, \boldsymbol{v}\circ T_t^{-1}, q\circ T_t^{-1}). \tag{3.11}$$

where the Lagrangian

$$G(\Omega_t, \boldsymbol{y}\circ T_t^{-1}, p\circ T_t^{-1}, \boldsymbol{v}\circ T_t^{-1}, q\circ T_t^{-1}) = I_1(t) + I_2(t) + I_3(t)$$

with

$$I_1(t) := 2\nu\int_{\Omega_t} |\varepsilon(\boldsymbol{y}\circ T_t^{-1})|^2\,\mathrm{d}x,$$

$$\begin{aligned} I_2(t) := -\int_{\Omega_t} [2\nu\varepsilon(\boldsymbol{v}\circ T_t^{-1}) : \varepsilon(\boldsymbol{y}\circ T_t^{-1}) + \mathrm{D}(\boldsymbol{y}\circ T_t^{-1})\cdot(\boldsymbol{y}\circ T_t^{-1})\cdot(\boldsymbol{v}\circ T_t^{-1})\\ - (p\circ T_t^{-1})\,\mathrm{div}\,(\boldsymbol{v}\circ T_t^{-1}) - (\boldsymbol{y}\circ T_t^{-1})\cdot\nabla(q\circ T_t^{-1})]\,\mathrm{d}x, \end{aligned}$$

and

$$I_3(t) := \int_{\Gamma_d} \boldsymbol{h}\cdot\boldsymbol{v}\,\mathrm{d}s.$$

Now we introduce the theorem concerning on the differentiability of a saddle point (or a minimax). To begin with, some notations are given as follows.

Define a functional

$$\mathcal{G} : [0,\tau]\times X\times Y\to\mathbb{R}$$

with $\tau > 0$, and X, Y are the two topological spaces.

For any $t \in [0,\tau]$, define $g(t) = \inf_{x\in X}\sup_{y\in Y}\mathcal{G}(t,x,y)$ and the sets

$$X(t) = \{x^t \in X : g(t) = \sup_{y\in Y}\mathcal{G}(t,x^t,y)\}$$
$$Y(t,x) = \{y^t \in Y : \mathcal{G}(t,x,y^t) = \sup_{y\in Y}\mathcal{G}(t,x,y)\}$$

Similarly, we can define the dual functional $h(t) = \sup_{y\in Y}\inf_{x\in X}\mathcal{G}(t,x,y)$ and the corresponding sets

$$Y(t) = \{y^t \in Y : h(t) = \inf_{x\in X}\mathcal{G}(t,x,y^t)\}$$
$$X(t,y) = \{x^t \in X : \mathcal{G}(t,x^t,y) = \inf_{x\in X}\mathcal{G}(t,x,y)\}$$

Furthermore, we introduce the set of saddle points

$$S(t) = \{(x,y) \in X \times Y : g(t) = \mathcal{G}(t,x,y) = h(t)\}$$

Now we can introduce the following theorem (see [5] or page 427 of [6]):

Theorem 3.1 *Assume that the following hypothesis hold:*

(H1) $S(t) \neq \emptyset,\ t \in [0,\tau]$;

(H2) The partial derivative $\partial_t\mathcal{G}(t,x,y)$ *exists in* $[0,\tau]$ *for all*

$$(x,y) \in \left[\bigcup_{t\in[0,\tau]} X(t)\times Y(0)\right]\bigcup\left[X(0)\times\bigcup_{t\in[0,\tau]} Y(t)\right];$$

(H3) There exists a topology $\mathcal{T}_X$ *on* X *such that for any sequence* $\{t_n : t_n \in [0,\tau]\}$ *with* $\lim_{n\nearrow\infty} t_n = 0$, *there exists* $x^0 \in X(0)$ *and a subsequence* $\{t_{n_k}\}$, *and for each* $k \geq 1$, *there exists* $x_{n_k} \in X(t_{n_k})$ *such that*

(i) $\lim_{n\nearrow\infty} x_{n_k} = x^0$ *in the* $\mathcal{T}_X$ *topology,*

(ii) $\liminf_{\substack{t\searrow 0\\ k\nearrow\infty}} \partial_t\mathcal{G}(t,x_{n_k},y) \geq \partial_t\mathcal{G}(0,x^0,y), \quad \forall y \in Y(0);$

(H4) There exists a topology $\mathcal{T}_Y$ *on* Y *such that for any sequence* $\{t_n : t_n \in [0,\tau]\}$ *with* $\lim_{n\nearrow\infty} t_n = 0$, *there exists* $y^0 \in Y(0)$ *and a subsequence* $\{t_{n_k}\}$, *and for each* $k \geq 1$, *there exists* $y_{n_k} \in Y(t_{n_k})$ *such that*

(i) $\lim_{n\nearrow\infty} y_{n_k} = y^0$ *in the* $\mathcal{T}_Y$ *topology,*

(ii) $\limsup_{\substack{t\searrow 0\\ k\nearrow\infty}} \partial_t\mathcal{G}(t,x,y_{n_k}) \leq \partial_t\mathcal{G}(0,x,y^0), \quad \forall x \in X(0).$

Then there exists $(x^0,y^0) \in X(0)\times Y(0)$ *such that*

$$\begin{aligned}\mathrm{d}g(0) &= \lim_{t\searrow 0}\frac{g(t)-g(0)}{t}\\ &= \inf_{x\in X(0)}\sup_{y\in Y(0)}\partial_t\mathcal{G}(0,x,y) = \partial_t\mathcal{G}(0,x^0,y^0) = \sup_{y\in Y(0)}\inf_{x\in X(0)}\partial_t\mathcal{G}(0,x,y)\end{aligned} \quad (3.12)$$

This means that $(x^0,y^0) \in X(0)\times Y(0)$ *is a saddle point of* $\partial_t\mathcal{G}(0,x,y)$.

Following Theorem 3.1, we need to differentiate the perturbed Lagrange functional $G(\Omega_t, \boldsymbol{y}\circ T_t^{-1}, p\circ T_t^{-1}, \boldsymbol{v}\circ T_t^{-1}, q\circ T_t^{-1})$.

To perform the differentiation, we introduce the following Hadamard formula[12]

$$\frac{\mathrm{d}}{\mathrm{d}t}\int_{\Omega_t} F(t,x)\,\mathrm{d}x = \int_{\Omega_t}\frac{\partial F}{\partial t}(t,x)\,\mathrm{d}x + \int_{\partial\Omega_t} F(t,x)\,\boldsymbol{V}\cdot\boldsymbol{n}_t\,\mathrm{d}s, \tag{3.13}$$

for a sufficiently smooth functional $F:[0,\tau]\times\mathbb{R}^N\to\mathbb{R}$.

By Hadamard formula (3.13), we get

$$\partial_t G(\Omega_t, \boldsymbol{y}\circ T_t^{-1}, p\circ T_t^{-1}, \boldsymbol{v}\circ T_t^{-1}, q\circ T_t^{-1}) = I_1'(0)+I_2'(0)+I_3'(0)+I_4'(0),$$

where

$$I_1'(0) = 4\nu\int_\Omega \varepsilon(\boldsymbol{y}):\varepsilon(-\mathrm{D}\boldsymbol{y}\cdot\boldsymbol{V})\,\mathrm{d}x + 2\nu\int_{\Gamma_s}|\varepsilon(\boldsymbol{y})|^2\boldsymbol{V}_n\,\mathrm{d}s; \tag{3.14}$$

$$\begin{aligned} I_2'(0) = -\int_\Omega &[2\nu\varepsilon(-\mathrm{D}\boldsymbol{y}\cdot\boldsymbol{V})\cdot\varepsilon(\boldsymbol{v}) + 2\nu\varepsilon(\boldsymbol{y})\cdot\varepsilon(-\mathrm{D}\boldsymbol{v}\cdot\boldsymbol{V}) + \mathrm{D}\boldsymbol{y}\cdot\boldsymbol{y}\cdot(-\mathrm{D}\boldsymbol{y}\cdot\boldsymbol{V})\\ &+\mathrm{D}(-\mathrm{D}\boldsymbol{y}\cdot\boldsymbol{V})\cdot\boldsymbol{y}\cdot\boldsymbol{v} + \mathrm{D}\boldsymbol{y}\cdot(-\mathrm{D}\boldsymbol{y}\cdot\boldsymbol{V})\cdot\boldsymbol{v} - p\,\mathrm{div}\,(-\mathrm{D}\boldsymbol{v}\cdot\boldsymbol{V})\\ &-\mathrm{div}\,(-\mathrm{D}\boldsymbol{y}\cdot\boldsymbol{V})q - \mathrm{div}\,\boldsymbol{y}(-\nabla q\cdot\boldsymbol{V}) - (-\nabla p\cdot\boldsymbol{V})\,\mathrm{div}\,\boldsymbol{v}]\,\mathrm{d}x\\ &+\int_{\Gamma_s}(-2\nu\varepsilon(\boldsymbol{y}):\varepsilon(\boldsymbol{v}) - \mathrm{D}\boldsymbol{y}\cdot\boldsymbol{y}\cdot\boldsymbol{v} + p\,\mathrm{div}\,\boldsymbol{v} + \mathrm{div}\,\boldsymbol{y}q)\boldsymbol{V}_n\,\mathrm{d}s; \end{aligned} \tag{3.15}$$

and $I_3'(0)=0$.

To simplify (3.14) and (3.15), we introduce the following lemma.

Lemma 3.2 *If two vector functions $\boldsymbol{y}$ and $\boldsymbol{v}$ vanish on the boundary Γ_s and $\mathrm{div}\,\boldsymbol{y} = \mathrm{div}\,\boldsymbol{v} = 0$ in Ω, the following identities*

$$\mathrm{D}\boldsymbol{y}\cdot\boldsymbol{V}\cdot\boldsymbol{n} = (\mathrm{D}\boldsymbol{y}\cdot\boldsymbol{n}\cdot\boldsymbol{n})\boldsymbol{V}_n = \mathrm{div}\,\boldsymbol{y}\boldsymbol{V}_n; \tag{3.16}$$

$$\varepsilon(\boldsymbol{y}):\varepsilon(\boldsymbol{v}) = \varepsilon(\boldsymbol{y}):(\varepsilon(\boldsymbol{v})\cdot(\boldsymbol{n}\otimes\boldsymbol{n})) = (\varepsilon(\boldsymbol{y})\cdot\boldsymbol{n})\cdot(\varepsilon(\boldsymbol{v})\cdot\boldsymbol{n}); \tag{3.17}$$

$$(\varepsilon(\boldsymbol{y})\cdot\boldsymbol{n})\cdot(\mathrm{D}\boldsymbol{v}\cdot\boldsymbol{V}) = (\varepsilon(\boldsymbol{y})\cdot\boldsymbol{n})\cdot(\mathrm{D}\boldsymbol{v}\cdot\boldsymbol{n})\boldsymbol{V}_n = (\varepsilon(\boldsymbol{y})\cdot\boldsymbol{n})\cdot(\varepsilon(\boldsymbol{v})\cdot\boldsymbol{n})\boldsymbol{V}_n \tag{3.18}$$

hold on the boundary Γ_s, where the tensor product $\boldsymbol{n}\otimes\boldsymbol{n} := \sum_{i,j=1}^N n_i n_j$.

Using Lemma 3.1, for (3.14) we have

$$I_1'(0) = -2\nu\int_\Omega \Delta\boldsymbol{y}\cdot(-\mathrm{D}\boldsymbol{y}\cdot\boldsymbol{V})\,\mathrm{d}x + 4\nu\int_{\Gamma_s}(\varepsilon(\boldsymbol{y})\cdot\boldsymbol{n})\cdot(-\mathrm{D}\boldsymbol{y}\cdot\boldsymbol{V})\,\mathrm{d}s + 2\nu\int_{\Gamma_s}|\varepsilon(\boldsymbol{y})|^2\boldsymbol{V}_n\,\mathrm{d}s.$$

By the identities (3.17) and (3.18), we further get

$$I_1'(0) = -2\nu\int_\Omega \Delta\boldsymbol{y}\cdot(-\mathrm{D}\boldsymbol{y}\cdot\boldsymbol{V})\,\mathrm{d}x - 2\nu\int_{\Gamma_s}|\varepsilon(\boldsymbol{y})|^2\boldsymbol{V}_n\,\mathrm{d}s. \tag{3.19}$$

Employing Lemma 3.1 and $\boldsymbol{y}|_{\Gamma_s} = \boldsymbol{V}|_{\Gamma_w \cup \Gamma_u \cup \Gamma_d} = 0$, (3.15) can be rewritten as

$$\begin{aligned} I_2'(0) = &\int_\Omega [(\nu\Delta\boldsymbol{y} - \mathrm{D}\boldsymbol{y}\cdot\boldsymbol{y} - \nabla p)\cdot(-\mathrm{D}\boldsymbol{v}\cdot\boldsymbol{V}) + \operatorname{div}\boldsymbol{y}(-\nabla q\cdot\boldsymbol{V})]\,\mathrm{d}x \\ &+ \int_\Omega [(\nu\Delta\boldsymbol{v} + \mathrm{D}\boldsymbol{v}\cdot\boldsymbol{y} - {}^*\mathrm{D}\boldsymbol{y}\cdot\boldsymbol{v} - \nabla q)\cdot(-\mathrm{D}\boldsymbol{y}\cdot\boldsymbol{V}) + \operatorname{div}\boldsymbol{v}(-\nabla p\cdot\boldsymbol{V})]\,\mathrm{d}x \\ &- \int_{\Gamma_s} [\sigma(\boldsymbol{y},p)\cdot\boldsymbol{n}\cdot(-\mathrm{D}\boldsymbol{v}\cdot\boldsymbol{V}) + \sigma(\boldsymbol{v},q)\cdot\boldsymbol{n}\cdot(-\mathrm{D}\boldsymbol{y}\cdot\boldsymbol{V})]\,\mathrm{d}s \\ &- \int_{\Gamma_s} [2\nu\varepsilon(\boldsymbol{y}):\varepsilon(\boldsymbol{v}) + \mathrm{D}\boldsymbol{y}\cdot\boldsymbol{y}\cdot\boldsymbol{v} - p\operatorname{div}\boldsymbol{v} - \operatorname{div}\boldsymbol{y}q]\boldsymbol{V}_n\,\mathrm{d}s. \end{aligned} \tag{3.20}$$

Since $(\boldsymbol{y},p)$ and $(\boldsymbol{v},q)$ satisfy (2.2)(2.3) and (3.5)(3.6) respectively, (3.20) reduces to

$$\begin{aligned} I_2'(0) = &2\nu\int_\Omega \Delta\boldsymbol{y}\cdot(-\mathrm{D}\boldsymbol{y}\cdot\boldsymbol{V})\,\mathrm{d}x \\ &- \int_{\Gamma_s} [\sigma(\boldsymbol{y},p)\cdot\boldsymbol{n}\cdot(-\mathrm{D}\boldsymbol{v}\cdot\boldsymbol{V}) + \sigma(\boldsymbol{v},q)\cdot\boldsymbol{n}\cdot(-\mathrm{D}\boldsymbol{y}\cdot\boldsymbol{V}) + 2\nu\varepsilon(\boldsymbol{y}):\varepsilon(\boldsymbol{v})\boldsymbol{V}_n]\,\mathrm{d}s. \end{aligned} \tag{3.21}$$

On the boundary Γ_s, we can deduce that

$$\begin{aligned} &-\sigma(\boldsymbol{y},p)\cdot\boldsymbol{n}\cdot(-\mathrm{D}\boldsymbol{v}\cdot\boldsymbol{V}) - \sigma(\boldsymbol{v},q)\cdot\boldsymbol{n}\cdot(-\mathrm{D}\boldsymbol{y}\cdot\boldsymbol{V}) \\ &= 2\nu[\varepsilon(\boldsymbol{y})\cdot\boldsymbol{n}\cdot(\mathrm{D}\boldsymbol{v}\cdot\boldsymbol{V}) + \varepsilon(\boldsymbol{v})\cdot\boldsymbol{n}\cdot(\mathrm{D}\boldsymbol{y}\cdot\boldsymbol{V})] && \text{(by (3.16))} \\ &= 4\nu(\varepsilon(\boldsymbol{y})\cdot\boldsymbol{n})\cdot(\varepsilon(\boldsymbol{v})\cdot\boldsymbol{n})\boldsymbol{V}_n && \text{(by (3.18))} \\ &= 4\nu\varepsilon(\boldsymbol{y}):\varepsilon(\boldsymbol{v})\boldsymbol{V}_n. && \text{(by (3.17))} \end{aligned}$$

Therefore, (3.21) becomes

$$I_2'(0) = 2\nu\int_\Omega \Delta\boldsymbol{y}\cdot(-\mathrm{D}\boldsymbol{y}\cdot\boldsymbol{V})\,\mathrm{d}x + 2\nu\int_{\Gamma_s}\varepsilon(\boldsymbol{y}):\varepsilon(\boldsymbol{v})\boldsymbol{V}_n\,\mathrm{d}s. \tag{3.22}$$

Adding (3.19) and (3.22) together, we finally obtain the boundary expression for the Eulerian derivative of $J(\Omega)$,

$$\mathrm{d}J(\Omega;\boldsymbol{V}) = 2\nu\int_{\Gamma_s}\left[\varepsilon(\boldsymbol{y}):\varepsilon(\boldsymbol{v}) - |\varepsilon(\boldsymbol{y})|^2\right]\boldsymbol{V}_n\,\mathrm{d}s, \tag{3.23}$$

Since the mapping $\boldsymbol{V}\mapsto \mathrm{d}J(\Omega;\boldsymbol{V})$ is linear and continuous, we get the expression for the shape gradient

$$\nabla J = 2\nu[\varepsilon(\boldsymbol{y}):\varepsilon(\boldsymbol{v}) - |\varepsilon(\boldsymbol{y})|^2]\boldsymbol{n} \tag{3.24}$$

by (2.1).

4 Finite element approximations and numerical Simulation

4.1 Discretization of the optimization problem

We suppose that Ω is a bounded polygonal domain of $\mathbb{R}^2$ and only consider the conforming finite element approximations. Let $X_h \subset H^1(\Omega)^N$ and $S_h \subset L^2(\Omega)$ be two

families of finite dimensional subspaces parameterized by h which tends to zero. We also define

$$\begin{aligned} V_{gh} &:= \{\boldsymbol{u}_h \in X_h :\ \boldsymbol{u}_h = 0 \text{ on } \Gamma_w \cup \Gamma_s,\ \boldsymbol{u}_h = \boldsymbol{g} \text{ on } \Gamma_u\}, \\ V_{0h} &:= \{\boldsymbol{u}_h \in X_h :\ \boldsymbol{u}_h = 0 \text{ on } \Gamma_w \cup \Gamma_u \cup \Gamma_s\}, \\ Q_h &:= \left\{ p_h \in S_h :\ \int_\Omega p_h \,\mathrm{d}x = 0 \ (\text{ if } \mathrm{meas}(\Gamma_d) = 0) \right\}. \end{aligned}$$

Besides, the following assumptions are supposed to hold.

(HA1) There exists $C > 0$ such that for $0 \le m \le l$,

$$\inf_{\boldsymbol{v}_h \in V_{gh}} \|\boldsymbol{v}_h - \boldsymbol{v}\|_1 \le C h^m \|\boldsymbol{v}\|_{m+1}, \qquad \forall \boldsymbol{v} \in H^{m+1}(\Omega)^N \cap V_g(\Omega);$$

(HA2) There exists $C > 0$ such that for $0 \le m \le l'$,

$$\inf_{q_h \in Q_h} \|q_h - q\|_0 \le C h^m \|q\|_m, \quad \forall q \in H^m(\Omega) \cap Q(\Omega);$$

(HA3) The Ladyzhenskaya-Brezzi-Babuska inf-sup condition is verified, i.e., there exists $C > 0$, such that

$$\inf_{0 \ne q_h \in Q_h} \sup_{0 \ne \boldsymbol{v}_h \in V_h} \frac{\int_\Omega q_h \,\mathrm{div}\, \boldsymbol{v}_h \,\mathrm{d}x}{\|\boldsymbol{v}_h\|_1 \|q_h\|_0} \ge C, \qquad V_h = V_{gh} \text{ or } V_{0h}.$$

The Galerkin finite element approximations of the state system (3.1) and adjoint state system (3.9) in mixed form are as follows

$$\begin{cases} \text{seek } (\boldsymbol{y}_h, p_h) \in V_{gh} \times Q_h \text{ such that } \forall (\boldsymbol{v}_h, q_h) \in V_{0h} \times Q_h, \\ \int_\Omega [2\nu \varepsilon(\boldsymbol{y}_h) : \varepsilon(\boldsymbol{v}_h) + \mathrm{D}\boldsymbol{y}_h \cdot \boldsymbol{y}_h \cdot \boldsymbol{v}_h - p_h \,\mathrm{div}\, \boldsymbol{v}_h] \,\mathrm{d}x = \int_{\Gamma_d} \boldsymbol{h} \cdot \boldsymbol{v}_h \,\mathrm{d}s, \\ \int_\Omega \,\mathrm{div}\, \boldsymbol{y}_h q_h \,\mathrm{d}x = 0, \end{cases} \tag{4.1}$$

and

$$\begin{cases} \text{seek } (\boldsymbol{v}_h, q_h) \in V_{0h} \times Q_h \text{ such that } \forall (\boldsymbol{\varphi}_h, \pi_h) \in V_{0h} \times Q_h, \\ \int_\Omega [2\nu \varepsilon(\boldsymbol{v}_h) : \varepsilon(\boldsymbol{\varphi}_h) + \mathrm{D}\boldsymbol{\varphi}_h \cdot \boldsymbol{y}_h \cdot \boldsymbol{v}_h + \mathrm{D}\boldsymbol{y}_h \cdot \boldsymbol{\varphi}_h \cdot \boldsymbol{v}_h - q_h \,\mathrm{div}\, \boldsymbol{\varphi}_h] \,\mathrm{d}x \\ \qquad\qquad = 4\nu \int_\Omega \varepsilon(\boldsymbol{y}_h) : \varepsilon(\boldsymbol{\varphi}_h) \,\mathrm{d}x, \\ \int_\Omega \,\mathrm{div}\, \boldsymbol{v}_h \pi_h \,\mathrm{d}x = 0. \end{cases} \tag{4.2}$$

We also have the discrete cost functional

$$J_h(\Omega) = 2 \int_\Omega |\varepsilon(\boldsymbol{y}_h)|^2 \,\mathrm{d}x, \tag{4.3}$$

and the discrete shape gradient

$$\nabla J_h = 2\nu [\varepsilon(\boldsymbol{y}_h) : \varepsilon(\boldsymbol{v}_h) - |\varepsilon(\boldsymbol{y}_h)|^2] \boldsymbol{n} \tag{4.4}$$

Finally for completeness, we state the following theorem (see [11]).

Theorem 4.1 *Assume that the hypotheses (HA1), (HA2) and (HA3) hold. Let*

$$\{(\lambda, (\boldsymbol{y}(\lambda), \lambda p(\lambda))); \lambda = 1/\nu \in \Lambda,\ \Lambda \text{ is a connected subsect of } \mathbb{R}^+\}$$

be a branch of nonsingular solutions of the state system (3.1). Then there exists a neighborhood $\mathcal{O}$ of the origin in $V_g(\Omega) \times Q(\Omega)$ and for $h \leq h_0$ sufficiently small a unique C^∞ branch $\{(\lambda, (\boldsymbol{y}_h(\lambda), \lambda p_h(\lambda))); \lambda \in \Lambda\}$ of nonsingular solutions of problem (4.1) such that

$$\lim_{h\to 0} \sup_{\lambda\in\Lambda} \{\|\boldsymbol{y}_h(\lambda) - \boldsymbol{y}(\lambda)\|_2 + \|p_h(\lambda) - p(\lambda)\|_1\} = 0.$$

In addition, for the adjoint state system (3.9) and its discrete form (4.2), we have the similar convergence result.

4.2 A gradient type algorithm

For the minimization problem (2.7), we rather work with the unconstrained minimization problem

$$\min_{\Omega\in\mathbb{R}^2} G(\Omega) = J(\Omega) + lV(\Omega), \tag{4.5}$$

where $V(\Omega) := \int_\Omega \mathrm{d}x$ and l is a positive Lagrange multiplier. The Eulerian derivative of $G(\Omega)$ is

$$\mathrm{d}G(\Omega; \boldsymbol{V}) = \int_{\Gamma_s} \nabla G \cdot \boldsymbol{V}\, \mathrm{d}s,$$

where the shape gradient $\nabla G := [2\nu\varepsilon(\boldsymbol{y}) : \varepsilon(\boldsymbol{v}) - 2\nu|\varepsilon(\boldsymbol{y})|^2 + l]\boldsymbol{n}$. Ignoring regularization, a descent direction is found by defining $\boldsymbol{V} = -h_k \nabla G$, and then we can update the shape Ω as $\Omega_k = (\mathrm{I} + h_k \boldsymbol{V})\Omega$, where h_k is a descent step at k-th iteration.

However, in this article in order to avoid boundary oscillations (and irregular shapes) and due to the fact that the gradient type algorithm produces shape variations which have less regularity than the original parametrization, we change the scalar product with respect to which we compute a descent direction, for instance, $H^1(\Omega)^2$. In this case, the descent direction is the unique element $\boldsymbol{d} \in H^1(\Omega)^2$ of the problem

$$\begin{cases} -\Delta \boldsymbol{d} + \boldsymbol{d} = 0 & \text{in } \Omega, \\ \boldsymbol{d} = 0, & \text{on } \Gamma_u \cup \Gamma_d \cup \Gamma_w, \\ \mathrm{D}\boldsymbol{d} \cdot \boldsymbol{n} = -\nabla G & \text{on } \Gamma_s. \end{cases} \tag{4.6}$$

To better understand the necessity of projection or smoother due to the loss of regularity, we give the following remark.

Remark 4.1 *We give a simple example to illustrate the loss of regularity. We suppose that the cost functional is a quadratic functional: $J(x) = (Ax - b)^2$ with $x \in H^1(\Omega)$, $A \in H^{-1}(\Omega)$ and $b \in L^2(\Omega)$. The gradient $\nabla J = 2(Ax - b)A \in H^{-1}(\Omega)$ has less regularity than x. Then any variation using ∇J as the descent direction will have less regularity than x, therefore we need to project into $H^1(\Omega)$. We refer the readers to see B.Mohammadi & O.Pironneau [14] and G.Dogan et.al.[7] for further discussion on regularity.*

The resulting algorithm can be summarized as follows:

(1) Choose an initial shape Ω_0, an initial step h_0 and a Lagrange multiplier l_0;

(2) Compute the state system (3.1) and the adjoint system (3.9), then we can evaluate the descent direction $\boldsymbol{d}_k$ by using (4.6) with $\Omega = \Omega_k$ and $l = l_k$;

(3) Set $\Omega_{k+1} = (\mathrm{I} + h_k \boldsymbol{d}_k)\,\Omega_k$ and $l_{k+1} = (l_k + l)/2 + \epsilon |V(\Omega_k) - V(\Omega)|/V(\Omega)$ with a small positive constant ϵ, where $l = -\int_{\Gamma_s} \nabla J \,\mathrm{d}s / \int_{\Gamma_s} \mathrm{d}s$ and $V(\Omega)$ is the given area of Ω.

The choice of the descent step size h_k is not an easy task. Too big, the algorithm is unstable; too small, the rate of convergence is insignificant. In order to refresh h_k, we compare h_k with h_{k-1}. If $(\boldsymbol{d}_k, \boldsymbol{d}_{k-1})_{H^1}$ is negative, we should reduce the step; on the other hand, if $\boldsymbol{d}_k$ and $\boldsymbol{d}_{k-1}$ are very close, we increase the step. In addition, if reversed triangles are appeared when moving the mesh, we also need to reduce the step.

In our algorithm, we do not choose any stopping criterion. A classical stopping criterion is to find that whether the shape gradients in some suitable norm is small enough. However, since we use the continuous shape gradients, it's hopeless for us to expect very small gradient norm because of numerical discretization errors. Instead, we fix the number of iterations. If it is too small, we can restart it with the previous final shape as the initial shape.

4.3 Numerical results

In all computations, the finite element discretization is effected using the P_1bubble–P_1 pair of finite element spaces on a triangular mesh, i.e., we choose the following velocity space X_h and pressure space S_h:

$$
\begin{aligned}
X_h &= \{\boldsymbol{y}_h \in (C^0(\bar{\Omega}))^2 : \boldsymbol{y}_h|_T \in (P_{1T}^*)^2, \forall T \in \mathcal{T}_h\} \\
S_h &= \{p_h \in C^0(\bar{\Omega}) : p_h|_T \in P_1, \forall T \in \mathcal{T}_h\},
\end{aligned}
$$

where $\mathcal{T}_h$ denotes a standard finite element triangulation of Ω, P_k the space of the polynomials in two variables of degree $\leq k$ and P_{1T}^* the subspace of P_3 defined by

$$
\begin{aligned}
P_{1T}^* = \{q : q = q_1 + \lambda \phi_T,\ &\text{with } q_1 \in P_1, \lambda \in \mathbb{R} \text{ and} \\
&\phi_T \in P_3, \phi_T = 0 \text{ on } \partial T,\ \phi_T(G_T) = 1 \text{ with } G_T \text{ is the centroid of } T\}.
\end{aligned}
$$

Notice that a function like ϕ_T is usually called a bubble function.

The mesh is performed by a Delaunay-Voronoi mesh generator (see [14]) and during the shape deformation, we utilize the a metric-based anisotropic mesh adaptation technique where the metric can be computed automatically from the Hessian of a solution. We run the programs on a home PC with Intel Pentium 4 CPU 2.8 GHz and 1GB memory.

4.3.1 Test case 1: cannula shape optimization in Stokes flow

We consider the shape optimization of a two-dimensional inflow cannula of a circulatory assist device in the biomedical applications. The geometry of the cannula Ω is depicted in the left picture of Figure 4.1. The boundary conditions for the problem are traction-free at the exit Γ_d, no-slip at all curved walls Γ_s, and a specified parabolic inlet velocity $\boldsymbol{g}(0, y) = ((y-2)(2.35-y), 0)^T$.

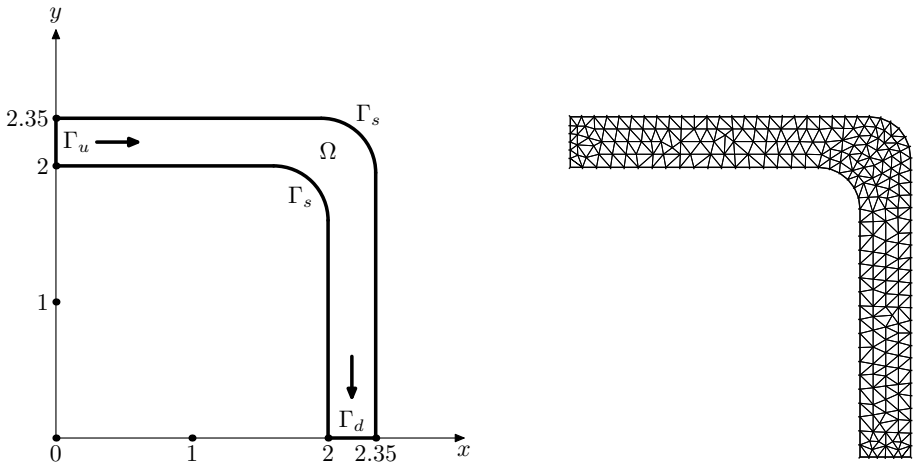

Figure 4.1: The analytic domain and the finite element mesh of the cannula.

In this test case, we present results for two different Reynolds numbers 0.1 and 0.01, defined as $\mathrm{Re} = d|\boldsymbol{y}_\mathrm{m}|/\nu$, where $\boldsymbol{y}_\mathrm{m}$ is the maximum velocity at the inlet Γ_u and $d = 0.35$ is the diameter of the cannula. The domain is discretized using 448 triangular elements and 279 nodes. Since the inertial term in (2.2) can be neglected when $\mathrm{Re} = 0.1$ or 0.01, we can say that the blood flow in the cannula was governed by the Stokes equations approximately.

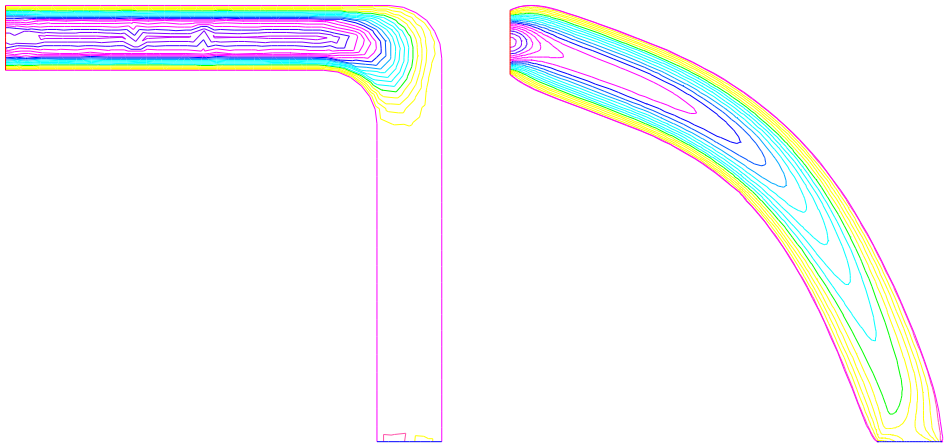

Figure 4.2: The initial and optimal cannula shapes with $\mathrm{Re} = 0.1$.

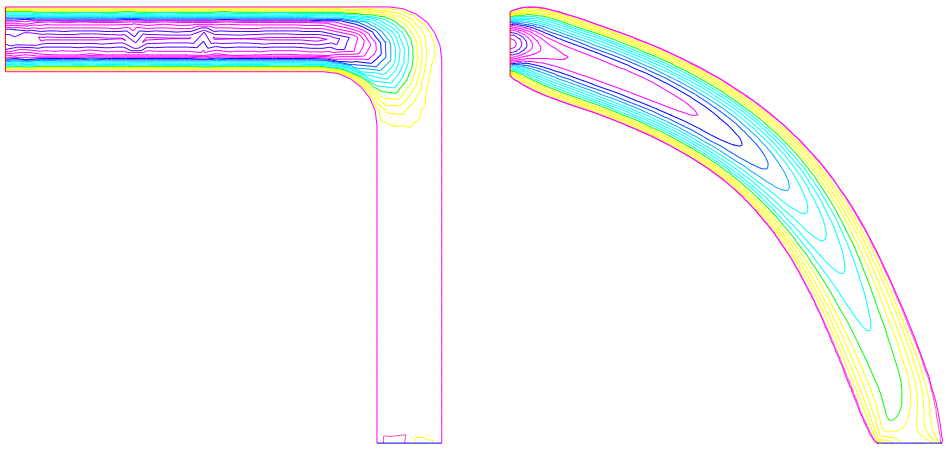

Figure 4.3: The initial and optimal cannula shapes with $\mathrm{Re} = 0.01$.

The distributions of the horizontal velocity for the initial and optimal shapes with $\mathrm{Re} = 0.1, 0.01$ are shown in Figure 4.2 and Figure 4.3. It is clear that shape optimization has removed the sharp bend in the initial configuration of the cannula.

The optimization process gave a 55.4975% reduction in the dissipated energy with $\mathrm{Re} = 0.1$, and a 55.0392% reduction in the dissipated energy with $\mathrm{Re} = 0.01$.

4.3.2 Test case 2: Optimization of a solid body in the Navier–Stokes flow

As a second test case, we consider the isolated body problem. The schematic geometry of the fluid domain is described in Figure 4.4, corresponding to an external flow around a solid body S. We reduce the problem to a bounded domain D by introducing an artificial boundary $\partial D := \Gamma_u \cup \Gamma_d \cup \Gamma_w$ which has to be taken sufficiently far from S so that the corresponding flow is a good approximation of the unbounded external flow around S and $\Omega := D \backslash \bar{S}$ is the effective domain. In addition, the boundary $\Gamma_s := \partial S$ is to be optimized.

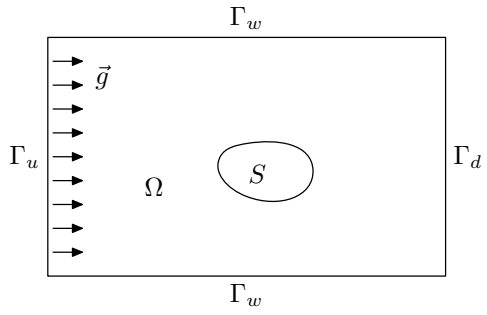

Figure 4.4: External flow around a solid body S.

We choose D to be a rectangle $(-0.5, 1.5) \times (-0.5, 1.5)$ and S is to be determined in our simulations. The inflow velocity is assumed to be parabolic with a profile

$\boldsymbol{g}(-0.5, y) = (0.2y^2 - 0.05, 0)^T$, while at the outflow boundary Γ_d, we impose a traction-free boundary condition ($\boldsymbol{h} = 0$). No-slip boundary condition are imposed at all the other boundaries. We further define the admissible set

$$\mathcal{O} := \left\{ \Omega \subset \mathbb{R}^2 : \ \partial D \text{ is fixed, the area } V(\Omega) = 1.9 \right\},$$

which means that the target volume of S to be optimized is 0.1.

We choose the initial shape of the body S to be a circle of center $(0, 0)$ with radius $r = 0.2$. We present results for two different Reynolds numbers $\mathrm{Re} = 40, 200$ defined by $\mathrm{Re} = 2r|\boldsymbol{y}_{\mathrm{m}}|/\nu$, where $\boldsymbol{y}_{\mathrm{m}}$ is the maximum velocity at the inflow Γ_u. The finite element mesh used for the calculations at $\mathrm{Re} = 200$ has been shown in Figure 4.5.

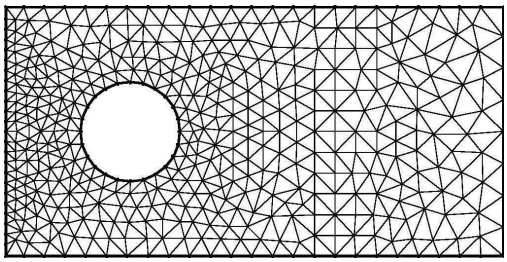

Figure 4.5: the finite element mesh.

Figure 5.6 and Figure 5.7 represent the distribution of the velocity $\boldsymbol{y} = (y_1, y_2)^T$ and the pressure p for the initial shape and the optimal shape in the neighborhood of S for $\mathrm{Re} = 40, 200$ respectively.

We run many iterations in order to show the good convergence and stability properties of our algorithm, however it is clear that it has converged in a smaller number of iterations (see Figure 5.8 and Figure 5.9). For the Reynolds numbers 40 and 200, the total dissipated energy reduced about 34.47% and 44.46% respectively.

5 Conclusion

The minimization problem of total dissipated energy in the two dimensional Navier–Stokes flow with mixed boundary conditions involving pressure has been presented. We derived the structure of shape gradient for the cost functional by function space parametrization technique without the usual study of the derivative of the state. Though for the time being this technique lacks from a rigorous mathematical framework for the Navier–Stokes equations, a gradient type algorithm is effectively used for the minimization problem for various Reynolds numbers. Further research is necessary on efficient implementations for time–dependent Navier–Stokes flow and much more real problems in the industry.

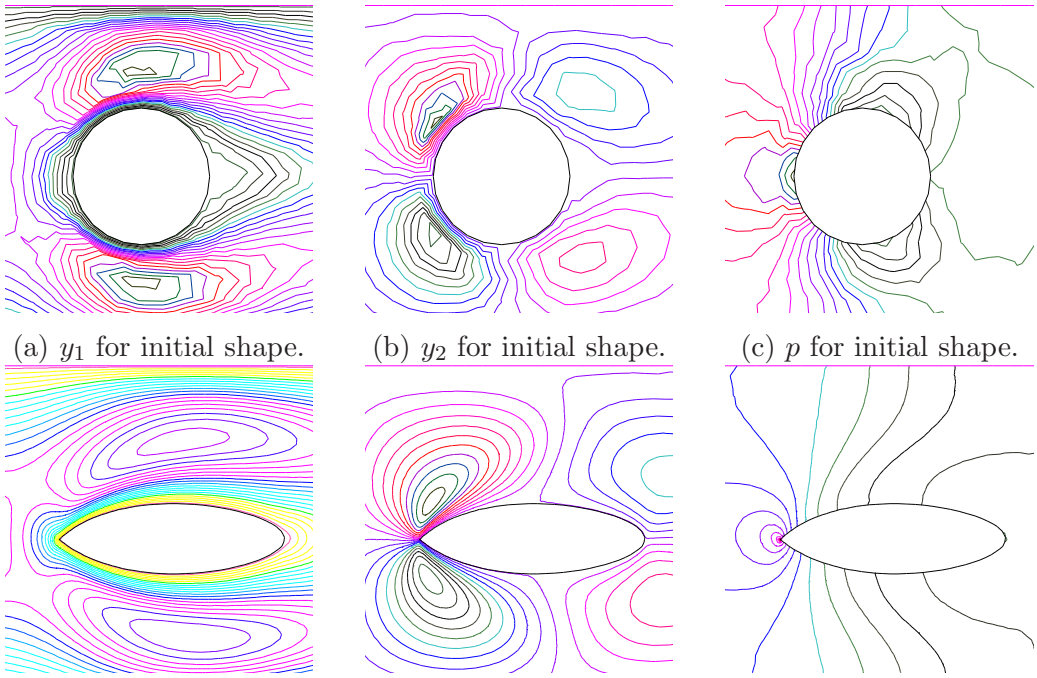

(a) y_1 for initial shape. (b) y_2 for initial shape. (c) p for initial shape.

(d) y_1 for optimal shape. (e) y_2 for optimal shape. (f) p for optimal shape.

Figure 5.6: Comparison of the initial shape and optimal shape for Re = 40.

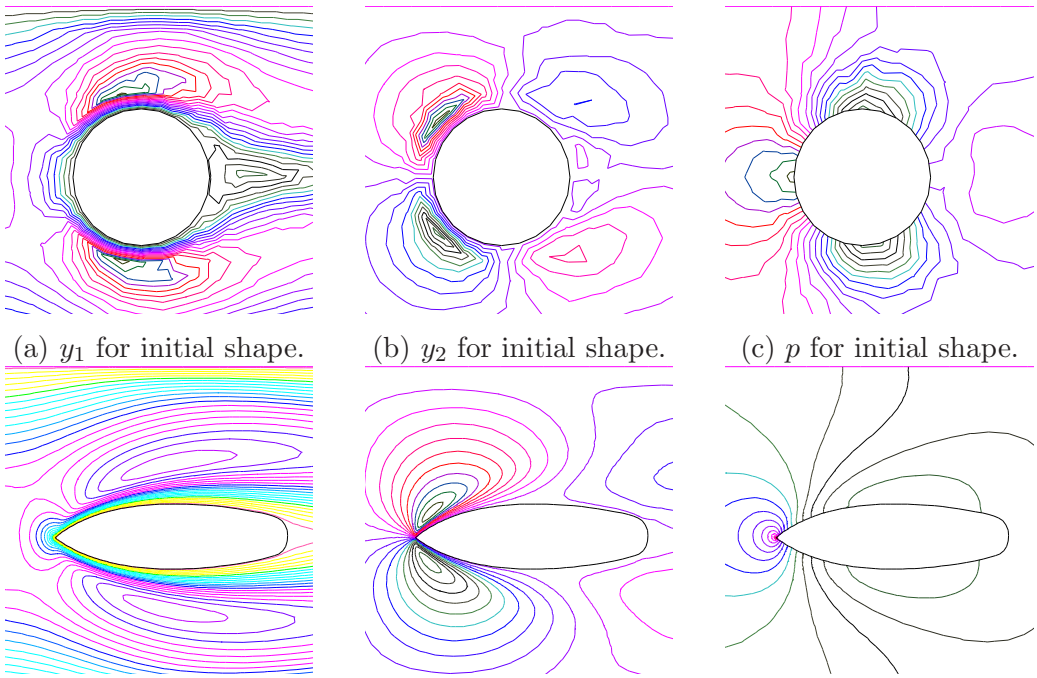

(a) y_1 for initial shape. (b) y_2 for initial shape. (c) p for initial shape.

(d) y_1 for optimal shape. (e) y_2 for optimal shape. (f) p for optimal shape.

Figure 5.7: Comparison of the initial shape and optimal shape for Re = 200.

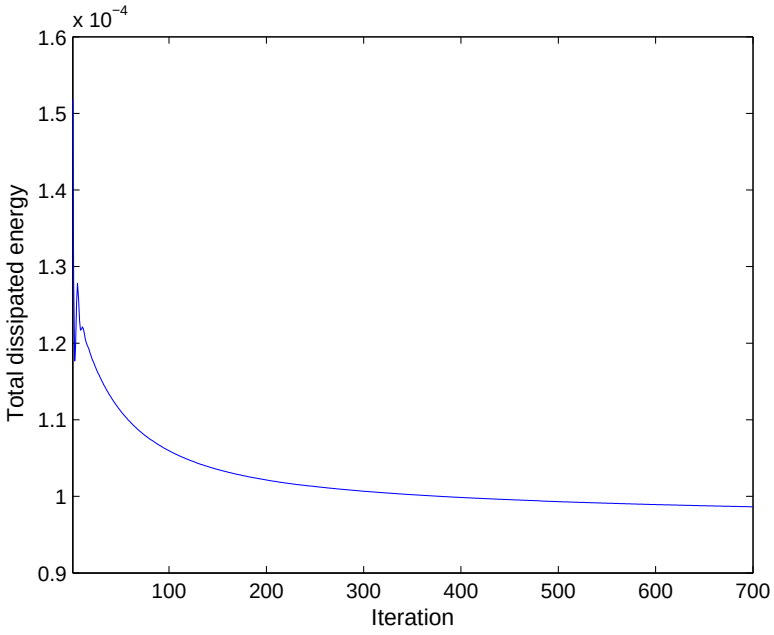

Figure 5.8: Convergence history of the total dissipated energy for Re = 40.

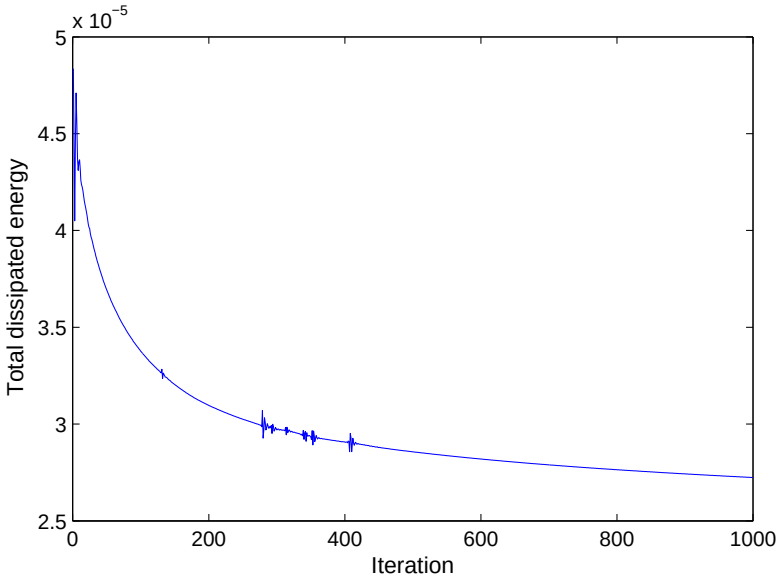

Figure 5.9: Convergence history of the total dissipated energy for Re = 200.

References

[1] J. Bello, E. Fernndez-Cara, J. Simon, Optimal shape design for navier-stokes flow, in: P. Kall (Ed.), System modelling and optimization, no. 180 in Lecture Notes in Control and Inform. Sci., Springer, 1992, pp. 481–489.

[2] J. Bello, E. Fernndez-Cara, J. Simon, The variation of the drag with respect to the domain in Navier-Stokes flow, in: Optimization, optimal control, partial differential equations, no. 107 in International Series of Numerical Mathematics, Birkhauser, 1992, pp. 287–296.

[3] J. Bello, E. Fernndez-Cara, J. Lemoine, J. Simon, The differentiability of the drag with respect to the variations of a lipschitz domain in a Navier-Stokes flow, SIAM Journal of Control and Optimization 35 (2) (1997) 626–640.

[4] J.Céa, Problems of shape optimal design, in: E.J.Haug, J.Céa (Eds.), Optimization of Distributed Parameter Structures, Vol. II, Sijthoff and Noordhoff, Alphen aan denRijn, 1981, pp. 1005–1048.

[5] R.Correa, A.Seeger, Directional derivative of a minmax function, Nonlinear Analysis, Theory Methods and Applications 9 (1985) 13–22.

[6] M.C.Delfour, J.-P.Zolésio, Shapes and Geometries: Analysis, Differential Calculus, and Optimization, Advance in Design and Control, SIAM, 2002.

[7] G.Dogan, P.Morin, R. H. Nochetto, M.Verani, Discrete gradient flows for shape optimization and applications, accepted in Computer Methods in Applied Mechanics and Engineering (2006).

[8] Z. Gao, Y. Ma, Shape sensitivity analysis for a Robin problem via minimax differentiability, Applied Mathematics and Computation 181 (2) (2006) 1090–1105.

[9] Z. Gao, Y. Ma, H. Zhuang, Optimal shape design for stokes flow via minimax differentiability, submitted.

[10] Z. Gao, Y. Ma, H. Zhuang, Shape optimization for Navier–Stokes flow, Preprint, http://arxiv.org/abs/math.OC/0612136 (2006).

[11] V.Girault, P.A.Raviart, Finite Element Methods for Navier-Stokes Equations, Springer-Verlag, 1986.

[12] J.Hadamard, Mémoire sur le problème d'analyse relatif à l'équilibre des plaques élastiques encastrées, in: Mémoire des savants étrangers, no. 33, 1907.

[13] E.Katamine, H.Azegami, T.Tsubata, S.Itoh, Solution to shape optimization problems of viscous flow fields, International Journal of Computational Fluid Dynamics 19 (1) (2005) 45–51.

[14] B.Mohammadi, O.Pironneau, Applied Shape optimization for fluids, Clardendon press, Oxford, 2001.

[15] F.Murat, J.Simon, Quelques resultats sur le controle par un domaine geometrique, Tech. Rep. 74003, Universite Paris VI., rapport du L.A. 189 (1974).

[16] O.Pironneau, Optimal Shape Design for Elliptic systems, Springer, Berlin, 1984.

[17] O.Pironneau, Optimal shape design by local boundary variations, in: B.Kawohl, O.Pironneau, L.Tartar (Eds.), Optimal shape design, Springer, 1988, lectures given at the joint C.I.M.

[18] J.Simon, Differentiation with respect to the domain in boundary value problems, Numer. Funct. Anal.Optim. 2 (1980) 649–687.

[19] R.Temam, Navier Stokes Equations, Theory and Numerical Analysis, ams chelsea edit. Edition, American Mathematical Society, Rhode Island, 2001.

[20] H.Yagi, M.Kawahara, Shape optimization of a body located in low reynolds number flow, International Journal for Numerical Methods in Fluids 48 (2005) 819–833.

[21] J.-P.Zolésio, Identification de domaines par déformation, Ph.D. thesis, Université de Nice (1979).